J. Fluid Mech. (1978), *vol.* 86, *part* 3, *pp.* 433–456
Printed in Great Britain

Thermal convection with spatially periodic boundary conditions: resonant wavelength excitation

By R. E. KELLY AND D. PAL
Mechanics and Structures Department, University of California, Los Angeles

(Received 27 June 1977)

Thermal convection in a fluid contained between two rigid walls with different mean temperatures is considered when either spatially periodic temperatures are prescribed at the walls or surface corrugations exist. The amplitudes of the spatial non-uniformities are assumed to be small, and the wavelength is set equal to the critical wavelength for the onset of Rayleigh–Bénard convection. For values of the mean Rayleigh number below the classical critical value, the mean Nusselt number and the mean flow are found as functions of Rayleigh number, Prandtl number, and modulation amplitude. For values of the Rayleigh number close to the classical critical value, the effects of the non-uniformities are greatly amplified, and the amplitude of convection is then governed by a cubic equation. This equation yields three supercritical states, but only the state linked to a subcritical state is found to be stable.

1. Introduction

In recent years, considerable interest has been shown in examining how the results of classical stability problems concerning steady flows contained between perfectly smooth boundaries are affected by temporal or spatial variations of the base state or boundaries. The recent review article by Davis (1976) gives information concerning the case when the variations are periodic in time. Not as much work has been done for the case when the variations are periodic in space, although the results would bear upon the importance of ignoring imperfections (e.g. roughness effects) when applying classical stability results to real situations, both in the laboratory and elsewhere.

The present analysis is aimed at examining the effects of spatially periodic boundary conditions upon the Rayleigh–Bénard stability problem (namely, an unstably stratified, Boussinesq fluid contained between two smooth, horizontal walls of infinite extent with constant but unequal temperatures). Two types of variation in the boundary conditions are considered, namely, (i) bounding surfaces which are plane but have temperatures which vary periodically (about different mean values) with distance along the surfaces, and (ii) surfaces which have constant but unequal temperatures and are wavy, so that the gap size varies periodically in a direction parallel to the mean surface levels.

Both cases are pertinent to stating how smooth conditions at a boundary must be in order that surface variations can be ignored in studies of thermal convection. The first case might also be relevant to estimating the extent to which well-defined initial disturbances (such as imposed by Chen & Whitehead 1968) affect stability boundaries,

etc., although our forcing is steady in time. The second case has some practical value in that one might want to make the boundary wavy if the mean Nusselt number could be increased (such a consideration seems to have motivated Watson & Poots (1971) in their study of how wavy boundaries affect laminar free convection flow between vertical walls).

In both cases, the amplitude of the variation (δ) is assumed to be small (in a sense to be defined more exactly later), and an expansion is made in terms of δ. The wavenumber (k) of the periodic variation is assumed to be close to or equal to the critical wavenumber ($k_c = 3{\cdot}117$) characteristic of classical Rayleigh–Bénard convection, and so we refer to the present problem as involving resonant wavelength excitation. Results for the situation when the wavenumber of the boundary modulation is significantly different from k_c will be reported elsewhere (Pal & Kelly 1978).

When no variations occur along the boundaries, convection is possible only when the Rayleigh number (Ra) is greater than the classical critical value ($Ra_c = 1707{\cdot}8$ for two rigid surfaces). When such variations do occur, convection occurs even though the Rayleigh number based on the mean values is less than Ra_c, and so the mean Nusselt number can vary with Ra. A mean flow can also be generated when a difference in phase is allowed between the variations occurring at the upper and lower boundaries, even though the forcing is stationary. That such a phenomenon is possible was suggested originally by Busse and Whitehead (see Busse 1972; Young, Schubert & Torrance 1972) during their studies of how *moving* thermal waves in an otherwise homogeneous fluid induce mean flows. We have calculated both mean Nusselt numbers and mean flow variations as functions of both Rayleigh and Prandtl numbers.

We have used the subscript c in the above to denote the values of the critical Rayleigh number and wavenumber for the classical problem with uniform heating. Strictly speaking, there is no critical Rayleigh number for the present problem in the usual sense because convection occurs for all values of Ra, and it should be borne in mind that the subscript c refers only to the numerical values associated with the classical problem. For $Ra \ll Ra_c$, however, the convection has an amplitude only of $O(\delta)$, and we shall refer to this regime as being that of 'quasi-conduction'. As Ra approaches Ra_c, the amplitude of convection increases greatly, however, and so it is still meaningful in a physical sense to define the 'critical' regime as being when $Ra \simeq Ra_c$.

One might expect that a solution based on expanding in terms of δ would become singular as $Ra \to Ra_c$ when $k = k_c$. This was confirmed in a preliminary report of our research (Kelly & Pal 1976) where it was shown by means of an eigenfunction expansion that

$$\epsilon \sim \delta Ra_c/(Ra_c - Ra). \tag{1.1}$$

A singularity was also noticed by Watson & Poots (1971) in their study of convection in a vertical slot as the Grashof number approaches the usual critical value (they also expanded in terms of δ). A singularity also exists in Busse's (1972) exact solution of the flow induced by internal heating in the form of a wave travelling between stress-free surfaces when one sets the frequency to zero, $k = k_c$, and $Ra = Ra_c$.

We demonstrated previously that when $Ra \simeq Ra_c$ nonlinear effects must be considered and that the scaling for the amplitude (ϵ) of convection can be determined from a model equation of the form

$$\epsilon^3 = \epsilon\{(Ra - Ra_c)/Ra_c C_2\} + \delta C_1, \tag{1.2}$$

where C_1 and C_2 are numerical constants (say, real and positive). For the quasi-conduction case when $Ra \ll Ra_c$ and $\delta \ll 1$, the linear terms in (1.2) give the same result as (1.1). For $\delta = 0$ and Ra slightly greater than Ra_c, (1.2) yields the well-known supercritical amplitude relation (Malkus & Veronis 1958)

$$\epsilon = \pm\{(Ra - Ra_c)/Ra_c C_2\}^{\frac{1}{2}}. \tag{1.3}$$

Hence (1.2) yields the two limiting cases. For $Ra = Ra_c$, it is clear from (1.2) that $\epsilon \sim O(\delta^{\frac{1}{3}})$ rather than zero as (1.3) states (or infinity, as (1.1) states). Relative to the quasi-conduction case when $\epsilon \sim O(\delta)$, we can say that the convection is now considerably enhanced. Taking $\epsilon \sim O(\delta^{\frac{1}{3}})$ as a standard for the critical regime, we note that each of the terms in (1.2) is of equal magnitude when

$$(Ra - Ra_c)/Ra_c \sim O(\delta^{\frac{2}{3}}), \tag{1.4}$$

which allows the critical regime to be defined more exactly. Of course, variation of the wavenumber away from the critical value will also affect the resonance phenomenon. An estimate of how close the wavenumber must be to the critical value is obtained by noting that the neutral curve for Rayleigh–Bénard convection behaves near Ra_c as

$$k - k_c \sim \pm\left(\frac{Ra - Ra_c}{Ra_c}\right)^{\frac{1}{2}}, \tag{1.5}$$

so that, by use of (1.4), we can say that resonance will occur within a neighbourhood of k_c defined by

$$k - k_c \sim O(\delta^{\frac{1}{3}}). \tag{1.6}$$

For the most part, we shall assume $k = k_c$. However, in order to show the effects of wavenumber variation, we shall occasionally give the results of a more general analysis of the case when $k \neq k_c$ but (1.6) holds. The details will be omitted, however, for the sake of brevity.

Our previous (1976) investigation gave a detailed analysis of the critical regime only for the case of stress-free surfaces, an infinite Prandtl number fluid, and a non-uniform boundary condition consisting of a single thermal wave imposed at the lower surface. Also, the nature of the solutions to the cubic equation (1.2) was not explored. The present report gives a much more complete analysis of this regime, including the effects of rigid boundaries, finite Prandtl number, and the phase angle between simultaneous forcing at the lower and upper boundaries. While this paper was being written, we received a preprint of the paper by Tavantzis, Reiss & Matkowsky (1978), in which their theory of singular perturbations (see Matkowsky & Reiss 1977) was used to obtain results in a more systematic manner for the general problem discussed here (they consider the case of a bounded layer with stress-free boundaries and a rather arbitrary variable temperature imposed on one boundary). Also, after this paper was originally submitted for publication, we were made aware of work by Daniels (1978) and Hall & Walton (1978) for the case of a bounded fluid layer with stress-free, constant temperature horizontal boundaries but with non-adiabatic end walls. Because this end-wall boundary condition can be viewed as being another kind of boundary imperfection, their results have qualitatively much in common with those reported by us and by Tavantzis *et al.*

2. Quasi-conduction regime

For Ra sufficiently below Ra_c so that (1.5) holds, we expect the amplitude of convection to be proportional to δ for $\delta \ll 1$. An analysis based on this premise is given in this section.

We measure distance in the horizontal and vertical directions by the variables x and z ($0 \leqslant z \leqslant 1$), respectively, which have been made non-dimensional on the basis of the average gap height H. If the mean temperature of the upper surface is $\overline{T}_u$ and that of the lower surface is $\overline{T}_l$, then the mean characteristic temperature difference is $\Delta\overline{T} = \overline{T}_l - \overline{T}_u$. We choose to scale the temperature on the basis of $\Delta\overline{T}$ as

$$T(x,z) = \Delta\overline{T}\tilde{\Theta}(x,z). \tag{2.1}$$

This means that we shall examine the effects of boundary modulation at a fixed value of $\Delta\overline{T}$ and that δ represents the magnitude of such variation relative to $\Delta\overline{T}$. This scaling is motivated by our basic interest in the effects of the boundary variations for the critical regime. The case with $\Delta\overline{T} = 0$ is discussed in the appendix.

We consider only two-dimensional convection because, for $Ra \ll Ra_c$, the convection is due only to the forcing at the boundaries, which is assumed to be periodic in the x direction. We therefore introduce a stream function $\psi(x,z)$ which we scale on the basis of the thermal diffusivity (κ) and δ as

$$\psi(x,z) = \kappa\tilde{\Psi}(x,z) = \kappa\delta\Psi(x,z). \tag{2.2}$$

For a boundary variation with a wavenumber k, it is convenient to use a new horizontal variable

$$\tilde{x} = kx. \tag{2.3}$$

We also define a temperature relative to the conduction state ($\delta = 0$) by

$$\tilde{\Theta}(\tilde{x},z) = (\overline{T}_l/\Delta\overline{T}) - z + \delta\Theta(\tilde{x},z). \tag{2.4}$$

For a Boussinesq fluid, the governing equations for Ψ and Θ are then

$$\frac{\partial^2\Theta}{\partial z^2} + k^2\frac{\partial^2\Theta}{\partial\tilde{x}^2} - k\frac{\partial\Psi}{\partial\tilde{x}} = k\delta\left(\frac{\partial\Psi}{\partial z}\frac{\partial\Theta}{\partial\tilde{x}} - \frac{\partial\Psi}{\partial\tilde{x}}\frac{\partial\Theta}{\partial z}\right), \tag{2.5}$$

and

$$\frac{\partial^4\Psi}{\partial z^4} + 2k^2\frac{\partial^4\Psi}{\partial z^2\partial\tilde{x}^2} + k^4\frac{\partial^4\Psi}{\partial\tilde{x}^4} - kRa\frac{\partial\Theta}{\partial\tilde{x}} = \frac{k\delta}{Pr}\left(\frac{\partial\Psi}{\partial z}\frac{\partial}{\partial\tilde{x}} - \frac{\partial\Psi}{\partial\tilde{x}}\frac{\partial}{\partial z}\right)\left(\frac{\partial^2\Psi}{\partial z^2} + k^2\frac{\partial^2\Psi}{\partial\tilde{x}^2}\right), \tag{2.6}$$

where Ra is a Rayleigh number based on $\Delta\overline{T}$ and H, and Pr is the Prandtl number.

The boundary conditions for each of the cases discussed in the introduction are as follows: (i) spatially periodic surface temperatures prescribed at plane rigid boundaries,

$$\Theta(\tilde{x},0) = (\overline{T}_l/\Delta\overline{T})\sin\tilde{x} = L\sin\tilde{x}, \tag{2.7a}$$

$$\Theta(\tilde{x},1) = (\overline{T}_u/\Delta\overline{T})\sin(\tilde{x}+\beta) = U\sin(\tilde{x}+\beta), \tag{2.7b}$$

$$\frac{\partial\Psi}{\partial\tilde{x}} = \frac{\partial\Psi}{\partial z} = 0 \quad \text{at} \quad z = 0,1, \tag{2.7c}$$

(ii) constant temperature wavy rigid boundaries,

$$\tilde{\Theta} = (\bar{T}_l/\Delta\bar{T}) \quad \text{at} \quad z = \zeta_l = \delta L \sin\tilde{x}, \tag{2.8a}$$

$$\tilde{\Theta} = (\bar{T}_u/\Delta\bar{T}) \quad \text{at} \quad z = \zeta_u = 1 + \delta U \sin(\tilde{x}+\beta), \tag{2.8b}$$

$$\frac{\partial\Psi}{\partial\tilde{x}} = \frac{\partial\Psi}{\partial z} = 0 \quad \text{at} \quad z = \zeta_l(\tilde{x}) \quad \text{and} \quad \zeta_u(\tilde{x}). \tag{2.8c}$$

In the above, β is a phase angle, and L and U are numerical constants to be prescribed later.

We now expand as

$$\Theta(\tilde{x},z) = \Theta_1(\tilde{x},z) + \delta\Theta_2(\tilde{x},z) + \ldots, \tag{2.9a}$$

and

$$\Psi(\tilde{x},z) = \Psi_1(\tilde{x},z) + \delta\Psi_2(\tilde{x},z) + \ldots, \tag{2.9b}$$

where the equations for Θ_1 and Ψ_1 are given by (2.5) and (2.6) with the right-hand sides set equal to zero. For case (i), the boundary conditions for Θ_1 and Ψ_1 are given by (2.7*a–c*). For case (ii), the conditions on Θ_1 and Ψ_1 can be obtained from (2.8*a–c*) by expanding $\tilde{\Theta}$ and Ψ about $z = 0$ and 1 in terms of δ, and then using (2.9*a*, *b*), as

$$\Theta_1(\tilde{x},0) = L\sin\tilde{x}, \quad \Theta_1(\tilde{x},1) = U\sin(\tilde{x}+\beta), \tag{2.10a}$$

$$\frac{\partial\Psi_1}{\partial\tilde{x}} = \frac{\partial\Psi_1}{\partial z} = 0 \quad \text{at} \quad z = 0, 1. \tag{2.10b}$$

Hence the boundary conditions are the same as in case (i) to order (δ).

We now redefine Θ_1 so as to obtain homogeneous boundary conditions; let

$$\Theta_1(\tilde{x},z) = \{\theta_{1l}(z) + L(1-z)\}\sin\tilde{x} + \{\theta_{1u}(z) + Uz\}\sin(\tilde{x}+\beta), \tag{2.11a}$$

and

$$\Psi_1(\tilde{x},z) = \Phi_{1l}(z)\cos\tilde{x} + \Phi_{1u}(z)\cos(\tilde{x}+\beta). \tag{2.11b}$$

With this notation, the subscript l denotes an effect associated with a variable lower-wall condition, whereas the subscript u denotes an effect caused by the upper wall.

The boundary conditions for both cases are then

$$\theta_{1l} = \theta_{1u} = 0 \quad \text{at} \quad z = 0, 1, \tag{2.12a}$$

$$\Phi_{1l} = \Phi_{1u} = 0 \quad \text{at} \quad z = 0, 1, \tag{2.12b}$$

$$\frac{d\Phi_{1l}}{dz} = \frac{d\Phi_{1u}}{dz} = 0 \quad \text{at} \quad z = 0, 1. \tag{2.12c}$$

The following inhomogeneous equations are obtained:

$$\frac{d^2\theta_{1l}}{dz^2} - k^2\theta_{1l} + k\Phi_{1l} = k^2L(1-z), \tag{2.13a}$$

$$\frac{d^4\Phi_{1l}}{dz^4} - 2k^2\frac{d^2\Phi_{1l}}{dz^2} + k^4\Phi_{1l} - kRa\theta_{1l} = kRaL(1-z), \tag{2.13b}$$

$$\frac{d^2\theta_{1u}}{dz^2} - k^2\theta_{1u} + k\Phi_{1u} = k^2Uz, \tag{2.14a}$$

$$\frac{d^4\Phi_{1u}}{dz^4} - 2k^2\frac{d^2\Phi_{1u}}{dz^2} + k^4\Phi_{1u} - kRa\theta_{1u} = kRaUz. \tag{2.14b}$$

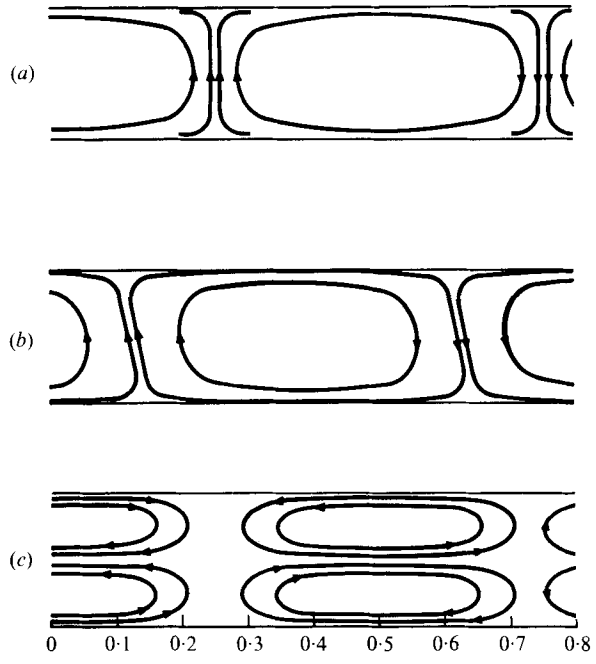

FIGURE 1. Streamlines of $O(\delta)$ convection cells for $Ra = 300, k = k_c = 2{\cdot}221$ (stress-free boundaries); (a) $\beta = 0°$, (b) $\beta = 90°$, (c) $\beta = 180°$.

At this point, an eigenfunction expansion was used by Kelly & Pal (1976) in order to clarify the situation as $Ra \to Ra_c$. The emphasis here is on calculating the $O(\delta)$ solution so as to be able then to calculate $O(\delta^2)$ mean quantities, and so the equations have been solved numerically. This has been done for $k = k_c$, the critical wavenumber for Rayleigh–Bénard convection. The streamlines show an interesting dependence upon the phase angle β, as shown in figures 1 (a)–(c) for $\beta = 0°$, 90° and 180°, respectively, and $L = U = 1$. Although these streamlines are actually for the stress-free boundary case, they are also representative of the rigid surface case. For $\beta = 0°$, closed cells appear with vertically oriented updrafts and downdrafts centred about the points of maximum and minimum wall temperatures, respectively. For $\beta = 90°$, a pronounced tilt occurs in the cells. This tilt leads to a non-zero Reynolds stress and so to the occurrence of a mean flow at $O(\delta^2)$. For $\beta = 180°$, it seems that a single cell cannot accommodate the boundary conditions, and a two-tier structure appears with two counter-rotating cells stacked on top of each other. For $\beta = 270°$, the streamlines would be similar to figure 1 (b), except that the tilt would be in the opposite direction.

At $O(\delta^2)$, the effects of the variable boundary conditions upon mean quantities, such as heat transfer, are determined. The mean temperature distortion is given by the solution of

$$\frac{d^2\overline{\Theta}_2}{dz^2} = -k\frac{d}{dz}\left(\overline{\Theta_1 \frac{\partial \Psi_1}{\partial \tilde{x}}}\right), \tag{2.15a}$$

where an overbar denotes an average over a wavelength. Upon substitution from (2.11 a) and (2.11 b), we get

$$\frac{d^2\overline{\Theta}_2}{dz^2} = \tfrac{1}{2}k\frac{d}{dz}[\Phi_{1l}\{\theta_{1l} + L(1-z)\} + \Phi_{1u}(\theta_{1u} + Uz) + \cos\beta\{\Phi_{1l}(\theta_{1u} + Uz) + \Phi_{1u}(\theta_{1l} + L(1-z))\}]. \tag{2.15b}$$

We note that the case $\beta = \frac{1}{2}\pi$ is special in that $\overline{\Theta}_2$ is then generated by the sum of terms forced by the lower wall plus terms forced by the upper wall (i.e. no interaction terms occur and only 'mean field' type terms remain).

The mean flow Ψ_2 is determined by

$$\frac{d^4\overline{\Psi}_2}{dz^4} = -\frac{k}{Pr}\frac{d^2}{dz^2}\left(\overline{\frac{\partial\Psi_1}{\partial\tilde{x}}\frac{\partial\Psi_1}{\partial z}}\right), \tag{2.16a}$$

or, after substituting from (2.11*b*),

$$\frac{d^4\overline{\Psi}_2}{dz^4} = \frac{k\sin\beta}{2Pr}\frac{d^2}{dz^2}\left\{\Phi_{1u}\frac{d\Phi_{1l}}{dz} - \Phi_{1l}\frac{d\Phi_{1u}}{dz}\right\}. \tag{2.16b}$$

The inhomogeneous quantity in (2.16*b*) is zero either if $\beta = 0$ or 180° or if L or U is zero (i.e. if one surface is isothermal). For all of these cases, the $O(\delta)$ convection cells have no tilt, and we can conclude immediately that no mean flow is generated, at least for the case of plane boundaries.

The boundary conditions for case (i) are

$$\overline{\Theta}_2 = \frac{d\overline{\Psi}_2}{dz} = 0 \quad \text{at} \quad z = 0, 1, \tag{2.17a}$$

$$\overline{\Psi}_2(0) = \overline{\Psi}_2(1) = 0. \tag{2.17b}$$

This last condition requires the volumetric flux to be zero, as would occur in a convection apparatus with closed ends. With this condition, the mean pressure gradient is also found to be zero.

The boundary conditions for case (ii) can be obtained by considering higher-order terms in the expansion of (2.8*a–c*) about the mean levels. However, this approach has the disadvantage that the mean velocity is then found to be non-zero at $z = 0$ and 1. This result is a natural consequence of the expansion procedure and occurs owing to inhomogeneous boundary terms arising at $O(\delta^2)$, as has been noted by Fung & Yih (1968) in their analysis of peristaltic transport. In order to present velocity profiles which vanish at the walls, we have introduced the transformation

$$\xi = (z - \zeta_l)/\zeta_T, \tag{2.18a}$$

where

$$\zeta_T = \zeta_u - \zeta_l, \tag{2.18b}$$

so that the walls are now located at $\xi = 0$ and 1. If we now take $\tilde{x}$ and ξ as independent variables, the conduction solution is given by $\{(\overline{T}_l/\Delta\overline{T}) - \xi\}$ and, if we let

$$\Theta_1(\tilde{x}, \xi) = \hat{\theta}_{1l}(\xi)\sin\tilde{x} + \hat{\theta}_{1u}(\xi)\sin(\tilde{x} + \beta), \tag{2.19}$$

the equations for $\hat{\theta}_{1l}(\xi)$ and $\hat{\theta}_{1u}(\xi)$ are found to be the same as the equations for $\theta_{1l}(z)$ and $\theta_{1u}(z)$, namely (2.13*a*) and (2.14*a*). $\Psi_1(\tilde{x}, \xi)$ is given by (2.11*b*), (2.13*b*), (2.14*b*), and the boundary conditions are as given in (2.12*a–c*), all with ξ substituted for z.

In the $\tilde{x}$, ξ plane, closed cells similar to those shown in figures 1(*a*)–(*c*), will occur at $O(\delta)$ but a mean current will be generated at $O(\delta^2)$ and can be obtained by averaging with respect to $\tilde{x}$ in this plane. The mean flow is governed by the equation

$$\frac{d^4\overline{\Psi}_2}{d\xi^4} = \frac{k\sin\beta}{2Pr}\frac{d^2}{d\xi^2}\left\{\Phi_{1u}\frac{d\Phi_{1l}}{d\xi} - \Phi_{1l}\frac{d\Phi_{1u}}{d\xi}\right\} + \frac{\sin\beta}{2}\frac{d^4}{d\xi^4}\left\{\xi U\frac{d\Phi_{1l}}{d\xi} - (1-\xi)L\frac{d\Phi_{1u}}{d\xi}\right\}. \tag{2.20}$$

We note that the inhomogeneous terms will be zero for case (ii) under the same conditions on β, L and U as given already for case (i). In comparing (2.20) with (2.16b), we note that, while $\bar{\Psi}_2$ in (2.16b) is produced solely by nonlinear advective terms proportional to Pr^{-1}, $\bar{\Psi}_2$ in (2.20) is also forced by terms arising from the variable geometry which are independent of Pr. This distinction in the forcing of the mean flows for the two cases remains true even after transforming back to the physical $\tilde{x}$, z plane for case (ii).

The equation for the mean temperature field in the $\tilde{x}$, ξ plane is

$$\begin{aligned}\frac{d^2\bar{\Theta}_2}{d\xi^2} = \frac{k}{2}\frac{d}{d\xi}[&\Phi_{1l}\{\theta_{1l}+L(1-\xi)\}+\Phi_{1u}(\theta_{1u}+U\xi)\\&+\cos\beta\{\Phi_{1l}(\theta_{1u}+U\xi)+\Phi_{1u}(\theta_{1l}+L(1-\xi))\}]\\&+\frac{L}{2}\frac{d^2}{d\xi^2}\left[(1-\xi)\frac{d}{d\xi}(\theta_{1l}+\cos\beta\theta_{1u})\right]\\&+\frac{U}{2}\frac{d^2}{d\xi^2}\left[\xi\frac{d}{d\xi}(\theta_{1u}+\cos\beta\theta_{1l})\right],\end{aligned} \tag{2.21}$$

which can be compared to (2.15b). The boundary conditions are

$$\bar{\Psi}_2 = \frac{d\bar{\Psi}_2}{d\xi} = \bar{\Theta}_2 = 0 \quad \text{at} \quad \xi = 0, 1. \tag{2.22}$$

For case (i), the mean heat transfer to the fluid at the lower boundary is

$$\bar{Q}(0) = -\frac{K}{H}\frac{d\bar{T}}{dz}\bigg|_{z=0} = \frac{K\Delta T}{H}\left[1-\delta^2\frac{d\bar{\Theta}_2}{dz}\bigg|_{z=0}+\ldots\right], \tag{2.23}$$

where K is the thermal conductivity. The mean Nusselt number is then, to $O(\delta^2)$,

$$\overline{Nu} = 1-\delta^2\frac{d\bar{\Theta}_2}{dz}\bigg|_{z=0}. \tag{2.24}$$

For case (ii), somewhat more care must be taken in defining $\overline{Nu}$ owing to the fact that the $\tilde{x}$, ξ co-ordinates are not orthogonal. If $\mathbf{n}$ is a unit vector normal to the lower boundary and pointing into the fluid, we have

$$\bar{Q}|_{z=\zeta_l} = -K\overline{\nabla T.\mathbf{n}}|_{z=\zeta_l}. \tag{2.25}$$

If we define $f = z-\zeta_l(x)$, then

$$\mathbf{n} = \frac{\nabla f}{|\nabla f|} = \frac{\mathbf{k}-\mathbf{i}(d\zeta_l/dx)}{\{1+(d\zeta_l/dx)^2\}^{\frac{1}{2}}}, \tag{2.26}$$

where $\mathbf{i}$ and $\mathbf{k}$ are unit vectors in the x and z directions, respectively. The local heat transfer rate is then

$$-Q|_{z=\zeta_l} = \frac{K/H}{\{1+k^2(d\zeta_l/d\tilde{x})^2\}^{\frac{1}{2}}}\left\{\frac{\partial T}{\partial z}-k^2\frac{d\zeta_l}{d\xi}\frac{\partial T}{\partial\tilde{x}}\right\}\bigg|_{z=\zeta_l}, \tag{2.27a}$$

or, using $\tilde{x}$ and ξ as variables,

$$-Q|_{\xi=0} = \frac{(K\Delta\bar{T}/H)}{\{1+k^2(d\zeta_l/d\tilde{x})^2\}^{\frac{1}{2}}}\left\{\frac{1}{\zeta_T}\frac{\partial\tilde{\Theta}}{\partial\xi}-k^2\frac{d\zeta_l}{d\tilde{x}}\left[\frac{\partial\tilde{\Theta}}{\partial\tilde{x}}-\frac{\partial\tilde{\Theta}}{\partial\xi}\frac{d}{d\tilde{x}}\left(\frac{\zeta_l}{\zeta_T}\right)\right]\right\}\bigg|_{\xi=0}. \tag{2.27b}$$

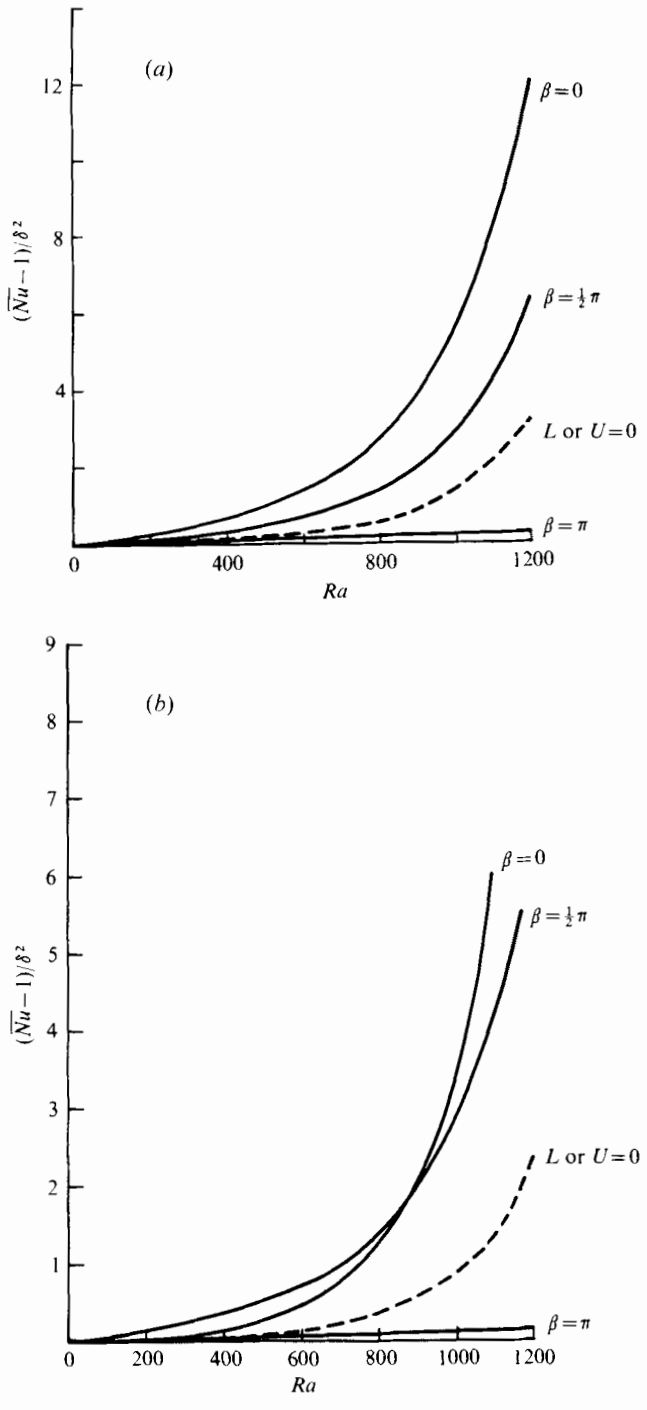

FIGURE 2. Mean Nusselt number at lower boundary as a function of Rayleigh number (Ra) and phase angle (β) with $k = k_c = 3{\cdot}117$; (*a*) case (i), (*b*) case (ii).

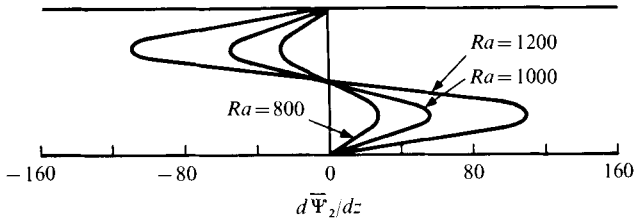

FIGURE 3. Mean velocity profiles at $O(\delta^2)$ for case (i) for $Pr = 0{\cdot}027$, $\beta = \frac{1}{2}\pi$ and various Rayleigh numbers.

After setting $\zeta_l = \delta L \sin\tilde{x}$, substituting the expansion of $\tilde{\Theta}$, and averaging, we get

$$\left.\frac{\bar{Q}H}{K\Delta\overline{T}}\right|_{\xi=0} = 1+\delta^2\left\{-\left.\frac{d\overline{\Theta}_2}{d\xi}\right|_{\xi=0} + \tfrac{1}{2}[U^2+L^2(1+\tfrac{1}{2}k^2)] - UL\cos\beta + \frac{\sin\beta}{2}\left(U\frac{d\theta_{1l}}{d\xi}+L\frac{d\theta_{1u}}{d\xi}\right)\right|_{\xi=0}\Bigg\}. \quad (2.28)$$

For case (i), the Nusselt number (2.24) approaches unity as $Ra \to 0$ because ψ_1 then tends to zero [cf. (2.13*b*), (2.14*b*)] and so also does $\overline{\Theta}_2$ [cf. (2.15)]. This occurs because we have scaled the boundary variation on the basis of $\Delta\overline{T}$ and so, as $\Delta\overline{T}\to 0$, the conduction state is obtained. For case (ii), a Nusselt number defined by (2.28) would not approach unity as $Ra \to 0$ because (2.28) then gives the heat transferred by conduction between wavy, rather than plane, boundaries. In order to present results for both cases in a uniform manner, we define a mean Nusselt number for case (ii) as

$$\overline{Nu} = (\bar{Q}H/K\Delta\overline{T})/(\bar{Q}H/K\Delta\overline{T})_{Ra=0}, \quad (2.29)$$

where $\bar{Q}$ is evaluated at $\xi = 0$.

Plots of $\overline{Nu}$, as defined by (2.24) and (2.29) to $O(\delta^2)$, are given in figures 2(*a*), (*b*) in terms of the quantity $(Nu-1)/\delta^2$ for various values of β and Ra. The solid curves are for $L = U = 1$, whereas the dashed curve is for $L = 1$, $U = 0$ (or vice versa). To $O(\delta^2)$, the results are independent of the Prandtl number. The mean heat transfer is strongly dependent upon Ra, even for $Ra \ll Ra_c = 1707{\cdot}8$. It is also strongly dependent upon β and for case (i) is clearly a maximum for $\beta = 0$ and a minimum for $\beta = \pi$. In the quasi-conduction regime, the heat transfer is proportional to the lowest-order motion induced by the horizontal temperature variation via the baroclinic effect. The vorticity generated by this means is proportional to $\nabla p \times \nabla T$, where the pressure p can be approximated at lowest order by the hydrostatic pressure. When this vector product has the same sign over most of a vertical section, the induced flow will be greatest and will affect $\overline{Nu}$ most strongly. Because ∇p is nearly a vector of constant magnitude pointing downwards for a Boussinesq fluid, $\partial T/\partial x$ should have the same sign over the range of z in order to maximize $\overline{Nu}$, i.e. the temperature variations should be in phase, as the numerical results given in figure 2(*a*) indicate. For case (ii), the situation is more complicated, and the phase angle for maximum $\overline{Nu}$ is found to be a function of Ra, as figure 2(*b*) indicates.

As might have been anticipated by the appearance of $\sin\beta$ in (2.16*b*), the mean flow is a maximum for case (i) when $\beta = \frac{1}{2}\pi$ or $\frac{3}{2}\pi$ for fixed Ra and Pr. The profile of the mean flow for case (i) is given in figure 3 for various values of Ra, $Pr = 0{\cdot}027$, and

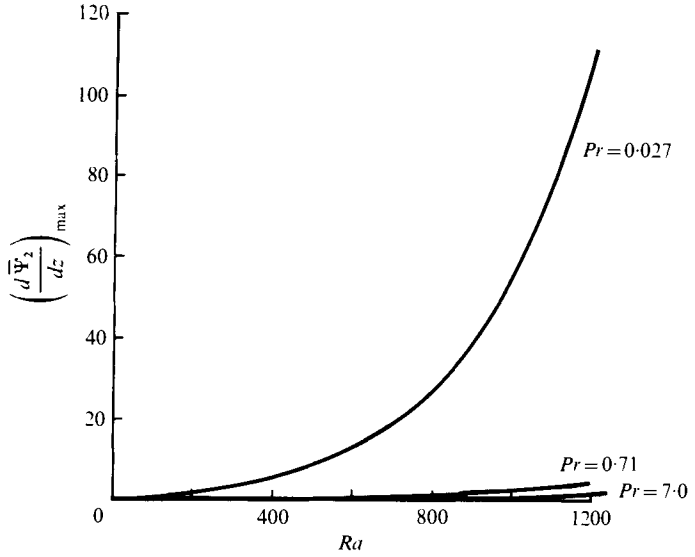

FIGURE 4. Maximum mean velocity at $O(\delta^2)$ for case (i) as a function of Rayleigh (Ra) and Prandtl (Pr) numbers.

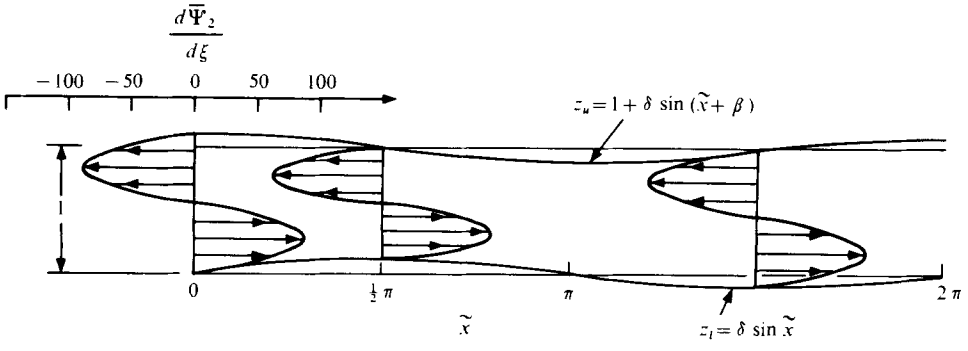

FIGURE 5. The open-ended circulatory flow at $O(\delta^2)$ for case (ii) for $\delta = 0{\cdot}1$, $\beta = 90°$, $Pr = 0{\cdot}025$ and $Ra = 1000$ ($k_c = 3{\cdot}117$).

$\beta = \frac{1}{2}\pi$. For $\beta = \frac{3}{2}\pi$, the sense of circulation should be reversed. As the figure indicates, the mean flow increases in magnitude as Ra increases. This is shown more clearly in figure 4, where the maximum value of $d\bar{\Psi}_2/dz$ is plotted as a function of Ra and Pr for case (i).

For case (ii), care needs to be taken in defining a 'mean' flow. In the strict sense, there is no absolutely x-independent flow, owing to the variation in height along the channel. However, we can ask how the mean flow in the x, ξ plane is transformed into an 'open-ended' but x-dependent cell in the x, z plane. This is done simply by plotting $d\bar{\Psi}_2/d\xi$, as obtained from (2.20), in the x, z plane by use of the relation

$$z = \zeta_l(x) + \zeta_T(x)\,\xi, \tag{2.30}$$

for constant ξ. A typical mean velocity distribution is given in figure 5 for $Pr = 0{\cdot}025$. Although the velocity maximum does not change with $\tilde{x}$, the profile becomes fuller as fluid moves into narrower regions. The maximum value of the 'mean' velocity is

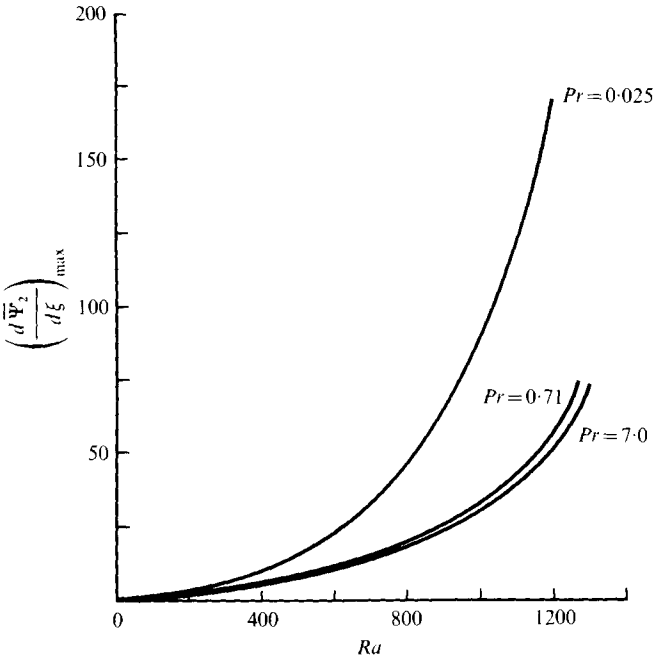

FIGURE 6. Maximum value of 'mean' velocity at $O(\delta^2)$ for case (ii) as a function of Rayleigh (Ra) and Prandtl (Pr) numbers.

shown in figure 6 as a function of Ra and Pr. The location of the maximum occurs closer to the wall as Pr increases. Note that typical values of the maximum streaming velocity are much larger in case (ii) than in case (i) for large Pr [cf. remarks after (2.20)].

3. The critical regime

We now consider the case when $k \simeq k_c = 3{\cdot}117$ and $Ra \simeq Ra_c = 1707{\cdot}8$. The scaling introduced heuristically in § 1 suggests the expansions

$$\tilde{\Theta}(x,z) = \Theta_0(z) + \delta^{\frac{1}{3}}\Theta_{\frac{1}{3}}(\tilde{x},z) + \delta^{\frac{2}{3}}\Theta_{\frac{2}{3}}(\tilde{x},z) + \delta\Theta_1(\tilde{x},z) + \ldots, \tag{3.1a}$$

$$\tilde{\Psi}'(\tilde{x},z) = \delta^{\frac{1}{3}}\Psi'_{\frac{1}{3}}(\tilde{x},z) + \delta^{\frac{2}{3}}\Psi'_{\frac{2}{3}}(\tilde{x},z) + \delta\Psi'_1(\tilde{x},z) + \ldots, \tag{3.1b}$$

$$Ra = Ra_c + \delta^{\frac{2}{3}}Ra_{\frac{2}{3}} + \ldots, \tag{3.1c}$$

and

$$k = k_c + \delta^{\frac{1}{3}}k_{\frac{1}{3}} + \ldots. \tag{3.1d}$$

Similar expansions have been developed by Tavantzis *et al.* (1978) in a more systematic manner, via the method of matched asymptotic expansions.

The expansion of the wavenumber (3.1*d*) allows us to investigate the effects of detuning the forcing within an $O(\delta^{\frac{1}{3}})$ range. Although some results will be given later in this regard, the actual equations become very complicated for $k \neq k_c$ and will be given only for $k = k_c$.

In (3.1*a*), Θ_0 is the conduction state for plane boundaries, and $\Theta_{\frac{1}{3}}$ and $\Theta_{\frac{2}{3}}$ correspond to solutions of the classical Rayleigh–Bénard stability problem, carried out to second order in the amplitude (i.e. the homogeneous boundary-value problem of Malkus & Veronis 1958). It seems unnecessary to present the details of that analysis; suffice it to say that we represent the solutions (with an asterisk denoting a complex conjugate) as

$$\Psi_{\frac{1}{3}}(\tilde{x},z) = \Phi_{\frac{1}{3}}(z)\,[A_{\frac{1}{3}}\exp(i\tilde{x}) + A_{\frac{1}{3}}^{*}\exp(-i\tilde{x})], \tag{3.2a}$$

$$\Theta_{\frac{1}{3}}(\tilde{x},z) = i\theta_{\frac{1}{3}}(z)\,[A_{\frac{1}{3}}\exp(i\tilde{x}) - A_{\frac{1}{3}}^{*}\exp(-i\tilde{x})], \tag{3.2b}$$

$$\Psi_{\frac{2}{3}}(\tilde{x},z) = -i\Phi_{\frac{2}{3}}(z)\,[(A_{\frac{1}{3}})^2\exp(2i\tilde{x}) - (A_{\frac{1}{3}}^{*})^2\exp(-2i\tilde{x})], \tag{3.2c}$$

and

$$\Theta_{\frac{2}{3}}(x,z) = \overline{\Theta}_{\frac{2}{3}}(z)|A_{\frac{1}{3}}|^2 + \theta_{\frac{2}{3}}(z)\,[(A_{\frac{1}{3}})^2\exp(2i\tilde{x}) + (A_{\frac{1}{3}}^{*})^2\exp(-2i\tilde{x})]. \tag{3.2d}$$

The equations for Θ_1 and Ψ_1 are then

$$\frac{\partial^2\Theta_1}{\partial z^2} + k_c^2\frac{\partial^2\Theta_1}{\partial\tilde{x}^2} - k_c\frac{\partial\Psi_1}{\partial\tilde{x}} = k_c\left\{\frac{\partial\Psi_{\frac{1}{3}}}{\partial z}\frac{\partial\Theta_{\frac{2}{3}}}{\partial\tilde{x}} + \frac{\partial\Psi_{\frac{2}{3}}}{\partial z}\frac{\partial\Theta_{\frac{1}{3}}}{\partial\tilde{x}} - \frac{\partial\Psi_{\frac{1}{3}}}{\partial\tilde{x}}\frac{\partial\Theta_{\frac{2}{3}}}{\partial z} - \frac{\partial\Psi_{\frac{2}{3}}}{\partial\tilde{x}}\frac{\partial\Theta_{\frac{1}{3}}}{\partial z}\right\}, \tag{3.3a}$$

and

$$\begin{aligned}\frac{\partial^4\Psi_1}{\partial z^4} + 2k_c^2\frac{\partial^4\Psi_1}{\partial z^2\,\partial\tilde{x}^2} + k_c^4\frac{\partial^4\Psi_1}{\partial\tilde{x}^4} - k_c Ra_c\frac{\partial\Theta_1}{\partial\tilde{x}} \\ = k_c Ra_{\frac{2}{3}}\frac{\partial\Theta_{\frac{1}{3}}}{\partial\tilde{x}} + \frac{k_c}{Pr}\left[\frac{\partial\Psi_{\frac{1}{3}}}{\partial z}\frac{\partial}{\partial\tilde{x}}\left(\frac{\partial^2\Psi_{\frac{2}{3}}}{\partial z^2} + k_c^2\frac{\partial^2\Psi_{\frac{2}{3}}}{\partial\tilde{x}^2}\right) + \frac{\partial\Psi_{\frac{2}{3}}}{\partial z}\frac{\partial}{\partial\tilde{x}}\left(\frac{\partial^2\Psi_{\frac{1}{3}}}{\partial z^2} + k_c^2\frac{\partial^2\Psi_{\frac{1}{3}}}{\partial\tilde{x}^2}\right)\right. \\ \left. - \frac{\partial\Psi_{\frac{1}{3}}}{\partial\tilde{x}}\frac{\partial}{\partial z}\left(\frac{\partial^2\Psi_{\frac{2}{3}}}{\partial z^2} + k_c^2\frac{\partial^2\Psi_{\frac{2}{3}}}{\partial\tilde{x}^2}\right) - \frac{\partial\Psi_{\frac{2}{3}}}{\partial\tilde{x}}\frac{\partial}{\partial z}\left(\frac{\partial^2\Psi_{\frac{1}{3}}}{\partial z^2} + k_c^2\frac{\partial^2\Psi_{\frac{1}{3}}}{\partial\tilde{x}^2}\right)\right].\end{aligned} \tag{3.3b}$$

The non-uniform boundary conditions appear only at this stage of the analysis and are the same as (2.7*a–c*) and (2.10*a–b*), namely,

$$\Theta_1(\tilde{x},0) = L\sin\tilde{x}, \quad \Theta_1(\tilde{x},1) = U\sin(\tilde{x}+\beta), \tag{3.4a}$$

$$\frac{\partial\Psi_{\frac{1}{3}}}{\partial\tilde{x}} = \frac{\partial\Psi_{\frac{1}{3}}}{\partial z} = 0 \quad \text{at} \quad z = 0, 1. \tag{3.4b}$$

To this order, therefore, the resonant solution does not depend on whether the non-uniformity arises from spatial temperature or gap variations.

We again redefine Θ_1 so as to obtain homogeneous boundary conditions; let

$$\Theta_1(\tilde{x},z) = \theta_1(\tilde{x},z) + (1-z)\,L\sin\tilde{x} + zU\sin(\tilde{x}+\beta). \tag{3.5}$$

If we let

$$\theta_1(\tilde{x},z) = i\theta_{11}(z)\exp(i\tilde{x}) + i\theta_{13}(z)\exp(3i\tilde{x}) + \text{complex conjugates}, \tag{3.6a}$$

$$\Psi_1(\tilde{x},z) = \Phi_{11}(z)\exp(i\tilde{x}) + \Phi_{13}(z)\exp(3i\tilde{x}) + \text{complex conjugates}, \tag{3.6b}$$

then the equations for θ_{11} and Φ_{11} are

$$\frac{d^2\theta_{11}}{dz^2} - k_c^2\theta_{11} - k_c\Phi_{11} = -\tfrac{1}{2}k_c^2(1-z)\,L - \tfrac{1}{2}k_c^2 zU\exp(i\beta) + k_c|A_{\frac{1}{3}}|^2A_{\frac{1}{3}}F(z), \tag{3.7a}$$

and

$$\left(\frac{d^2}{dz^2}-k_c^2\right)^2\Phi_{11}+k_c Ra_c\theta_{11}$$
$$=-k_c Ra_{\frac{2}{3}}A_{\frac{1}{3}}\theta_{\frac{1}{3}}+\tfrac{1}{2}k_c Ra_c[L(1-z)+Uz\exp(i\beta)]+k_c Pr^{-1}|A_{\frac{1}{3}}|^2A_{\frac{1}{3}}G(z), \tag{3.7b}$$

where

$$F(z)=2\frac{d\Phi_{\frac{1}{3}}}{dz}\theta_{\frac{2}{3}}+\frac{d\Phi_{\frac{2}{3}}}{dz}\theta_{\frac{1}{3}}+\Phi_{\frac{1}{3}}\frac{d\theta_{\frac{2}{3}}}{dz}+2\Phi_{\frac{2}{3}}\frac{d\theta_{\frac{1}{3}}}{dz}-\Phi_{\frac{1}{3}}\frac{d\bar{\Theta}_{\frac{2}{3}}}{dz}, \tag{3.7c}$$

and

$$G(z)=2\frac{d\Phi_{\frac{1}{3}}}{dz}\left(\frac{d^2\Phi_{\frac{2}{3}}}{dz^2}-4k_c^2\Phi_{\frac{2}{3}}\right)-\frac{d\Phi_{\frac{2}{3}}}{dz}\left(\frac{d^2\Phi_{\frac{1}{3}}}{dz^2}-k_c^2\Phi_{\frac{1}{3}}\right)$$
$$+\Phi_{\frac{1}{3}}\left(\frac{d^3\Phi_{\frac{2}{3}}}{dz^3}-4k_c^2\frac{d\Phi_{\frac{2}{3}}}{dz}\right)-2\Phi_{\frac{2}{3}}\left(\frac{d^3\Phi_{\frac{1}{3}}}{dz^3}-k_c^2\frac{d\Phi_{\frac{1}{3}}}{dz}\right). \tag{3.7d}$$

Consider the homogeneous adjoint system given by

$$\frac{d^2\hat{\theta}}{dz^2}-k_c^2\hat{\theta}-k_c Ra_c\hat{\Phi}=0, \tag{3.8a}$$

$$\left(\frac{d^2}{dz^2}-k_c^2\right)^2\hat{\Phi}+k_c\hat{\theta}=0, \tag{3.8b}$$

where

$$\hat{\theta}=\hat{\Phi}=\frac{d\hat{\Phi}}{dz}=0 \quad \text{at} \quad z=0,1. \tag{3.8c}$$

If we multiply (3.7*a*) by $\hat{\theta}(=\theta_{\frac{1}{3}})$, (3.7*b*) by $\hat{\Phi}(=\Phi_{\frac{1}{3}}/Ra_c)$, integrate both equations from $z=0$ to 1 and then subtract one resulting equation from the other, we obtain the following solvability condition:

$$k_c|A_{\frac{1}{3}}|^2A_{\frac{1}{3}}\left\{\int_0^1 F\hat{\theta}\,dz-Pr^{-1}\int_0^1 G\hat{\Phi}\,dz\right\}+k_c Ra_{\frac{2}{3}}A_{\frac{1}{3}}\int_0^1\theta_{\frac{1}{3}}\hat{\Phi}\,dz$$
$$=\tfrac{1}{2}k_c L\left\{k_c\int_0^1(1-z)\hat{\theta}\,dz+Ra_c\int_0^1(1-z)\hat{\Phi}\,dz\right\}$$
$$+\tfrac{1}{2}k_c U\exp(i\beta)\left\{k_c\int_0^1 z\hat{\theta}\,dz+Ra_c\int_0^1 z\hat{\Phi}\,dz\right\}. \tag{3.9}$$

By making use of the symmetry of $\hat{\theta}$ and $\hat{\Phi}$, it is easy to see that the terms in curly brackets on the right-hand side of (3.9) are equal. Hence, after evaluating the various integrals, and including now terms representing the wavenumber variation, we can express (3.9) as

$$A_{\frac{1}{3}}[I_1|A_{\frac{1}{3}}|^2-(Ra_{\frac{2}{3}}/Ra_c)+I_2(k_{\frac{1}{3}}/k_c)^2]=[L+U\exp(i\beta)]I_3, \tag{3.10}$$

where $I_2=1{\cdot}435$ and $I_3=0{\cdot}144$. Only I_1 is dependent upon Pr and ranges between a value of 13·05 for $Pr=\infty$ to 222·7 for $Pr=0{\cdot}027$. Various checks were made on the accuracy of the numerical computations. For instance, the linear terms on the left-hand side describe the shape of the known neutral curve near $Ra=Ra_c$, $k=k_c$. Also, for $k_{\frac{1}{3}}=L=U=0$, the remaining terms can be used to compute a Nusselt number, which was compared with the results given by Clever & Busse (1974). Finally, all the integrals were evaluated numerically for stress-free boundary conditions, for which

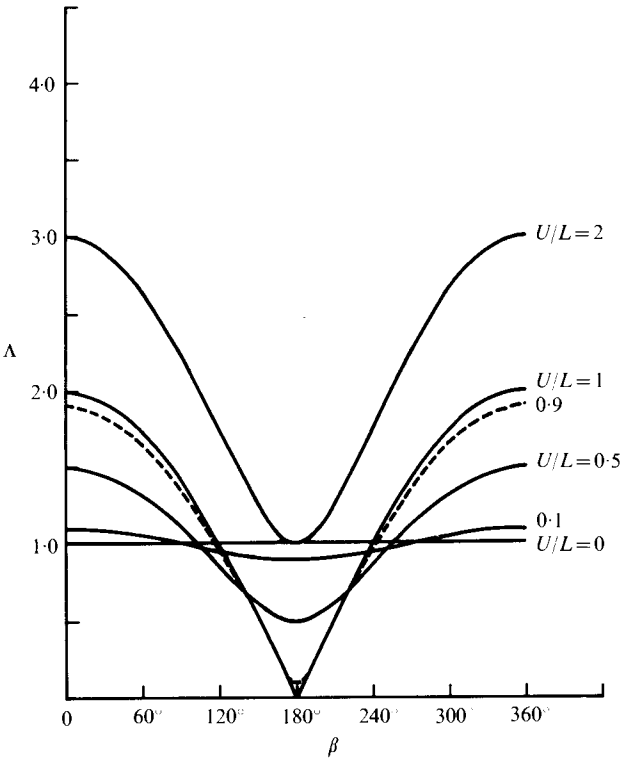

FIGURE 7. The dependence of the function Λ upon β and (U/L).

case an analytical solution is possible ($I_1 = \frac{3}{4}\pi^2$, $I_2 = \frac{4}{3}$ and $I_6 = \frac{2}{3}\pi$ for that case). Satisfactory agreement was found in all the comparisons.

We note for $L \neq 0$ that we can also write the complex term on the right-hand side of (3.10) as

$$L + U\exp(i\beta) = L\{1 + 2(U/L)\cos\beta + (U/L)^2\}^{\frac{1}{2}}\exp(i\lambda) \qquad (3.11a)$$

$$= L\Lambda\exp(i\lambda),$$

where

$$\tan\lambda = \frac{U\sin\beta}{L + U\cos\beta}. \qquad (3.11b)$$

For $\beta = 180°$ and $L = U$, $\Lambda = 0$, and the forcing drops out of the solvability condition (3.10). Hence, for equal amplitude but antisymmetric forcing, the forcing has no effect on the convection to the order considered. In order to investigate the general case, we let

$$A_{\frac{1}{3}} = \pm|A_{\frac{1}{3}}|\exp(i\lambda), \qquad (3.12)$$

and obtain the following relation for $|A_{\frac{1}{3}}|$:

$$\pm|A_{\frac{1}{3}}|[I_1|A_{\frac{1}{3}}|^2 - (Ra_{\frac{2}{3}}/Ra_c) + I_2(k_{\frac{1}{3}}/k_c)^2] = L\Lambda I_3. \qquad (3.13)$$

The $\pm$ sign is included because, for $L\Lambda = 0$, we have

$$|A_{\frac{1}{3}}|^2_{R-B} = I_1^{-1}\{(Ra_{\frac{2}{3}}/Ra_c) - I_2(k_{\frac{1}{3}}/k_c)^2\}, \qquad (3.14)$$

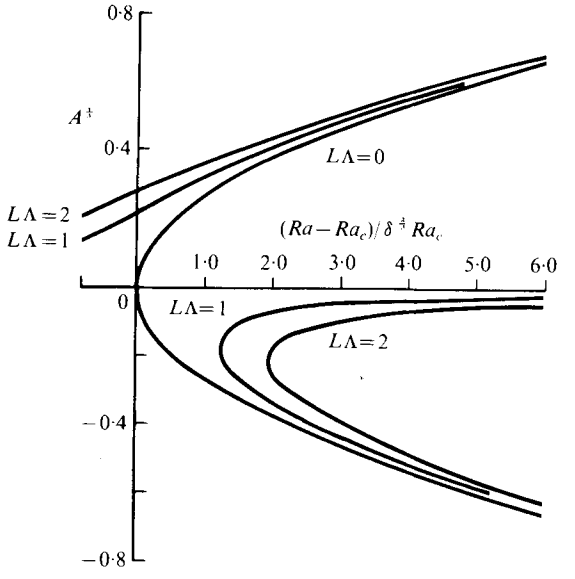

FIGURE 8. The amplitude of convection $A_{\frac{1}{3}}$ *vs.* $(Ra-Ra_c)/\delta^{\frac{2}{3}}Ra_c$ for infinite Prandtl number ($k = k_c = 3{\cdot}117$).

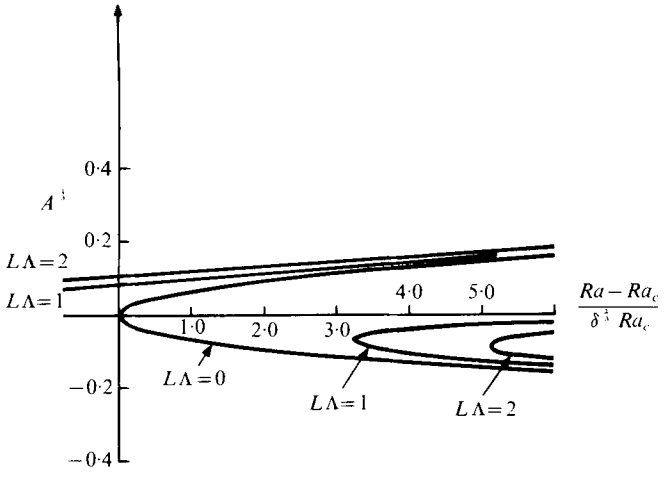

FIGURE 9. The amplitude of convection $A_{\frac{1}{3}}$ *vs.* $(Ra-Ra_c)/\delta^{\frac{2}{3}}Ra_c$ for $Pr = 0{\cdot}027$ ($k = k_c = 3{\cdot}117$).

and the minus sign simply represents a phase shift of 180° of the convection roll relative to the case of the plus sign. For $L\Lambda \neq 0$, it is clear that, with the plus sign, the amplitude $|A_{\frac{1}{3}}|$ is always greater for supercritical Ra_c than for the case with $L\Lambda = 0$, whereas the reverse is true for the minus sign. Say that we consider the case when $\beta = 0$ or $U = 0$. This result then says that the solution which is in phase with the forcing has a greater amplitude than a solution which is 180° out of phase, which seems quite reasonable. Note that the out-of-phase solution can exist only if $Ra > Ra_c$ for $L\Lambda \neq 0$.

We choose to plot $|A_{\frac{1}{3}}|$ as a function of $L\Lambda$, even though this parameter depends

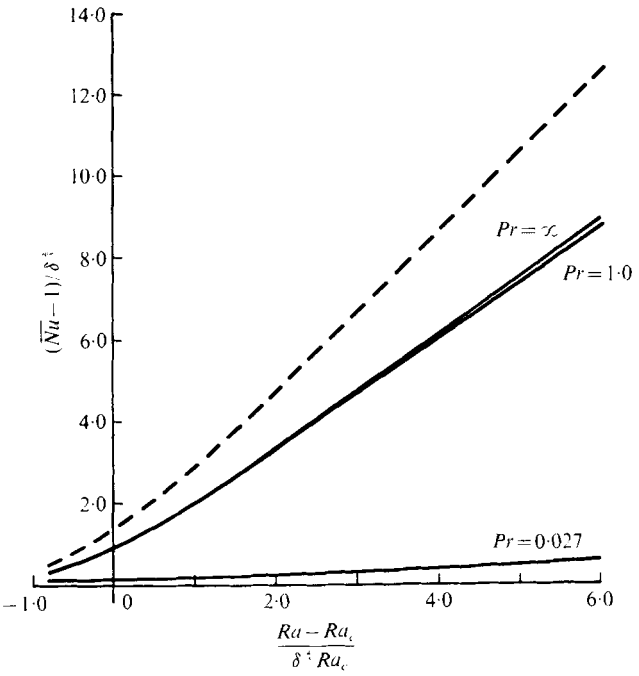

FIGURE 10. The Nusselt number near Ra_c for resonant forcing for $\Lambda L = 1$ and various Pr (dashed curve is for stress-free boundary case, all Pr).

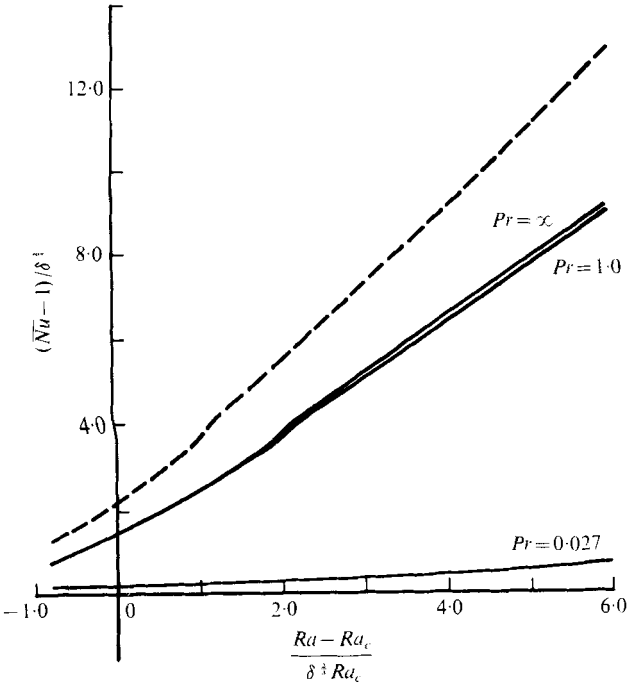

FIGURE 11. The Nusselt number near Ra_c for resonant forcing for $\Lambda L = 2$ and various Pr (dashed curve is for stress-free boundary case, all Pr).

upon L, U, and β, because it is an effective amplitude of forcing. The parameter Λ is shown as a function of U/L and β in figure 7. Although Λ is a minimum for all values of $U/L > 0$ at $\beta = 180°$, it is actually zero only for $U/L = 1$. It is a maximum always for $\beta = 0$ if $U \neq 0$; for $U = 0$, the effect of phase angle drops out, as it should.

Plots of $|A_{\frac{1}{3}}|$ as a function of the Rayleigh number and $L\Lambda$ are shown in figure 8 for $Pr = \infty$ and in figure 9 for $Pr = 0{\cdot}027$. These plots show clearly the features of the solutions discussed in the penultimate paragraph but also reveal that three solutions exist in general, a point to which we shall return shortly.

From an experimental viewpoint, the behaviour of the Nusselt number near $Ra = Ra_c$ with $\delta \neq 0$ is of special interest because a sudden change in the slope of the Nusselt number versus Rayleigh number curve is usually used as the criterion for the critical Rayleigh number. To the order considered, the mean Nusselt number at the lower boundary (for either case) is

$$\overline{Nu} = 1 - \delta^{\frac{2}{3}} \frac{d\bar{\Theta}_{\frac{2}{3}}}{dz} |A_{\frac{1}{3}}|^2 \Big|_{z=0}. \tag{3.15}$$

The quantity $(\overline{Nu} - 1)/\delta^{\frac{2}{3}}$ is plotted in figure 10 for $\Lambda L = 1$ (e.g. $L = 1$, $U = 0$) and in figure 11 for $\Lambda L = 2$ (e.g. $L = U = 1$, $\beta = 0°$) for various values of Pr, using the solution with the greatest amplitude. For $\Lambda L = 2$, $Pr = \infty$, and $\delta = 0{\cdot}01$, the Nusselt number at $Ra_c = 1707{\cdot}8$ is $1{\cdot}044$ versus unity for $\delta = 0$. Remembering that δ is a measure of the non-uniformity relative to $\Delta\bar{T}$ (which is usually of the order of a few degrees), we can see how non-uniformities can make a precise determination of Ra_c rather difficult in an experiment, owing to the amplification of small imperfections as $Ra \to Ra_c$. The actual non-uniformity could be more general than sinusoidal, and the present results would still apply, as long as the Fourier representation of the non-uniformity contains a component with $k = k_c$, as shown by Tavantzis *et al.* (1978). The amplitude of the Fourier component associated with k_c would then correspond to δ. In a carefully controlled experiment Ahlers (1975) has found a smooth transition of the type shown in figures 10 and 11.

The composite result for $\overline{Nu}$ obtained from the expansions for both the quasi-convection and critical regimes with $\delta = 0{\cdot}1$ is shown in figure 12. Again, the solution with the greatest amplitude is used. The curves for each regime merge smoothly. This figure suggests that one way of defining criticality in an experiment is to note the point at which the curvature of the Nusselt number curve changes sign. This would seem somewhat preferable to a criterion that the Nusselt number be above unity by some arbitrary amount.

We now return to the matter of the multiple solutions which can exist for sufficiently large Ra, as evidenced by figures 8 and 9. These figures can be viewed as giving a quasi-steady estimate of the amplitude of convection for given $L\Lambda$ as Ra increases slowly from $Ra < Ra_c$ to $Ra > Ra_c$. From this point of view, only the solution with the largest amplitude [corresponding to the positive sign in (3.13)] would seem at first to be the physically relevant solution, in the sense that only it can evolve from a subcritical state. We explored the matter by introducing a slow $O(\delta^{\frac{2}{3}})$ time scale into the amplitude equation and then solving for the time-dependent amplitude on the basis of an initial-value problem, as Ra increases with time. Even with initial conditions corresponding to negative $A_{\frac{1}{3}}$, the solution always evolved towards the upper curve in figures 8 and 9 as Ra approached Ra_c from below. Nonetheless, the other

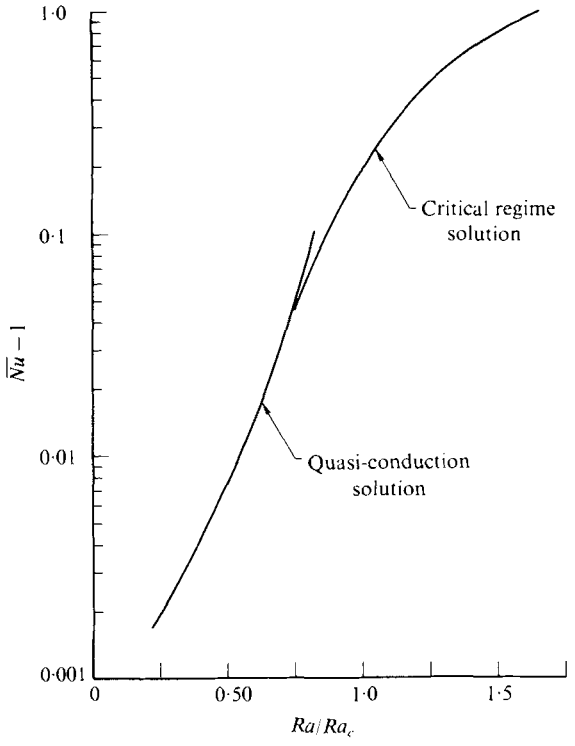

FIGURE 12. Composite Nusselt number curve for $\delta = 0{\cdot}1$, $\Lambda L = 1$, $k = k_c = 3{\cdot}117$.

solutions could occur if the evolving solution becomes unstable for Ra greater than Ra_c by some amount. For this reason, it is worth considering the relative stability of the solutions.

In order to investigate the matter, we introduce the slow time scale $\tau = \delta^{\frac{2}{3}}t$ and consider the equation [cf. (3.10)]

$$\frac{dA}{d\tau} = \sigma A - I_1 A|A|^2 + \hat{L}e^{i\lambda}, \tag{3.16}$$

where $\sigma = (Ra_{\frac{1}{3}}/Ra_c)$ and $\hat{L} = L\Lambda I_3$ are both understood to be real and positive and where the subscript $\frac{1}{3}$ has been dropped. If we let $A = \hat{A}\exp(i\lambda)$, the equilibrium states are given by

$$\hat{A}_e^3 - (\sigma/I_1)\hat{A}_e - (\hat{L}/I_1) = 0. \tag{3.17}$$

For $\hat{L} = 0$, we have the two non-trivial solutions $\hat{A}_{e,0} = \pm(\sigma/I_1)^2$. For $\hat{L} \neq 0$, knowledge of the characteristics of roots to a cubic equation allows us to say that three real, distinct roots exist if

$$(\sigma/3I_1)^3 > (\hat{L}/2I_1)^2, \tag{3.18}$$

which we assume to be true. By expanding in terms of $\hat{L}$ for $\hat{L}$ sufficiently small, we find that two of the solutions to (3.17) are

$$\hat{A}_{e,1} \simeq +\left(\frac{\sigma}{I_1}\right)^{\frac{1}{2}}\left\{1 + \frac{2LI_1^{\frac{1}{2}}}{\sigma^{\frac{3}{2}}}\right\}, \tag{3.19a}$$

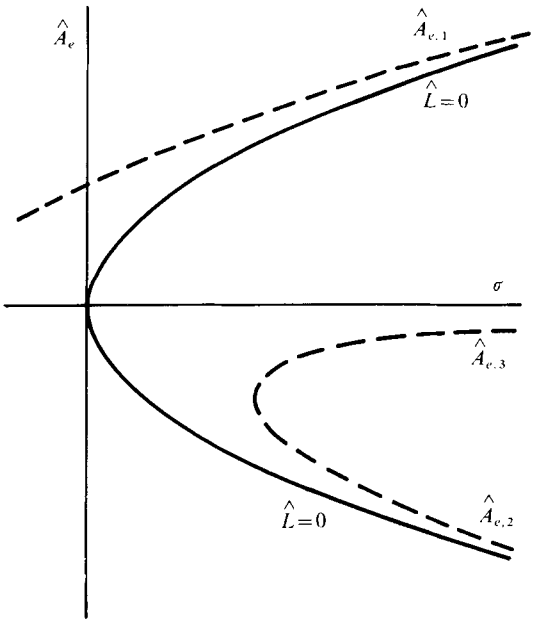

FIGURE 13. Schematic diagram of the three supercritical equilibrium solutions.

and

$$\hat{A}_{e,2} \simeq -\left(\frac{\sigma}{I_1}\right)^{\frac{1}{2}}\left\{1-\frac{2\hat{L}I_1^{\frac{1}{2}}}{\sigma^{\frac{3}{2}}}\right\}. \tag{3.19b}$$

Note that $|\hat{A}_{e,1}| > |\hat{A}_{e,0}|$ and $|\hat{A}_{e,2}| < |\hat{A}_{e,0}|$. The third solution corresponds to the conduction solution when $\hat{L} = 0$ and is

$$\hat{A}_{e,3} \simeq -\hat{L}/\sigma. \tag{3.19c}$$

The three possible solutions are sketched qualitatively in figure 13, which can be compared with figure 8.

In order to consider the stability of the equilibrium states, we let

$$A_j(\tau) = \hat{A}_{e,j}\exp(i\lambda) + a_j(\tau), \tag{3.20}$$

where $j = 1$, 2, or 3 and a_j is a small perturbation to the equilibrium state, which we take in the form $a_j = \hat{a}_j \exp(i\phi + \alpha\tau)$, where $\alpha = \alpha_r + i\alpha_i$. By substituting (3.20) into (3.16), linearizing the resulting equation, and collecting terms proportional to $\cos\alpha_i\tau$, we can obtain

$$\alpha_r = \sigma - I_1(\hat{A}_{e,j})^2\{1+2\cos^2(\lambda-\phi)\}, \tag{3.21a}$$

$$\alpha_i = I_1(\hat{A}_{e,j})^2 \sin 2(\phi-\lambda), \tag{3.21b}$$

whereas collecting terms proportional to $\sin\alpha_i\tau$ yields

$$\alpha_r = \sigma - I_1(\hat{A}_{e,j})^2\{1+2\sin^2(\lambda-\phi)\}, \tag{3.22a}$$

$$\alpha_i = I_1(\hat{A}_{e,j})^2 \sin 2(\lambda-\phi). \tag{3.22b}$$

Because $(\hat{A}_{e,1})^2 > (\hat{A}_{e,0})^2 = (\sigma/I_1)$, we obtain the result that $\alpha_r < 0$ for the disturbance a_1 for all values of λ and ϕ. Hence the solution corresponding to $\hat{A}_{e,1}$, i.e. the solution with the greatest amplitude, is stable, at least to a disturbance with the same wavenumber. In order to determine its overall stability, we must, of course, consider a

more general three-dimensional disturbance. Such an investigation would be part of determining the pattern of convection for $Ra > Ra_c$, and we hope to pursue this analysis in the future.

With regard to the solutions corresponding to $j = 2$ and 3, consider first the point at which they coalesce, i.e. when $(\sigma/3I_1)^3 = (\hat{L}/2I_1)^2$. At this point, one can easily show that

$$(\hat{A}_{e,2})^2 = (\hat{A}_{e,3})^3 = (\hat{L}/2I_1)^{\frac{3}{2}} = \sigma/3I_1. \tag{3.23}$$

From (3.21*a*), we have then

$$\alpha_r = \frac{2\sigma}{3}\{1 - \cos^2(\lambda - \phi)\}, \tag{3.24}$$

which says that the state is unstable as long as the disturbance is not in phase or 180° out of phase with the equilibrium state. An analogous result comes from consideration of (3.22*a*). For a larger value of σ, such that (3.18) is satisfied and $A_{e,2}$ is distinct from $A_{e,3}$, we have

$$(\hat{A}_{e,2})^2 > \sigma/3I_1, \quad (\hat{A}_{e,3})^2 < \sigma/3I_1. \tag{3.25}$$

We can conclude immediately that the solution corresponding to $\hat{A}_{e,3}$ is unstable for all values of ϕ because the growth rate of the disturbance a_3 is, according to (3.21*a*),

$$\alpha_r > \frac{2\sigma}{3}\{1 - \cos^2(\lambda - \phi)\} \geqslant 0. \tag{3.26}$$

With regard to $\hat{A}_{e,2}$, the maximum value of the growth rate corresponding to a_2 is

$$(\alpha_r)_{\max} = \sigma - I_1(\hat{A}_{e,2})^2. \tag{3.27}$$

Because $(\hat{A}_{e,2})^2 < (\hat{A}_{e,0})^2 = (\sigma/I_1)$, $(\alpha_r)_{\max} > 0$, and so the state $\hat{A}_{e,2}$ is also unstable. In contrast to the state $\hat{A}_{e,3}$, however, the phase of the disturbance is now of importance.

We can therefore conclude that the solution corresponding to $\hat{A}_{e,1}$ is the only stable equilibrium solution. Daniels (1978) has made a similar conclusion for the case with non-adiabatic end-wall boundary conditions.

The work of D. Pal has been supported in part by the U.C.L.A. Academic Senate and by an N.S.F. Energy Related Graduate Traineeship. R.E.K. is grateful to A. Craik for a helpful comment.

Appendix

As $Ra \to 0$ in (2.5) and (2.6), the equations become uncoupled. Because $\Psi \equiv 0$ is then the solution of (2.6), only the conduction solution can be obtained from (2.5) {which, of course, is zero for case (i)}. This uncoupling occurs because we scaled both the mean field and the forced field on the basis of $\Delta\overline{T}$. If the temperature modulation is held fixed as $\Delta\overline{T} \to 0$, then we must scale differently so that the equations remain coupled and retain the physics. The necessary transformation is

$$\Theta = (\overline{T}_b/\Delta\overline{T})\,\hat{\Theta}, \tag{A 1}$$

where $\overline{T}_b$ is some reference boundary temperature (say, $\overline{T}_l$ if $\overline{T}_u = 0$). When substituted

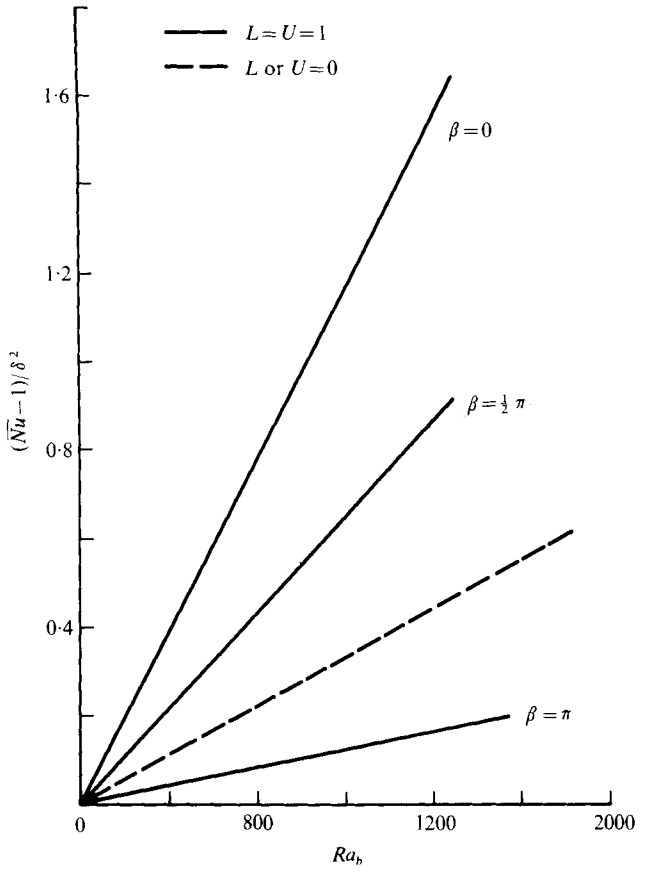

FIGURE 14. Mean Nusselt number for $\Delta\bar{T} = 0$ as a function of Rayleigh number Ra_b based on reference boundary temperature and phase angle β for $k = 3{\cdot}117$; solid lines are for $\bar{T}_l = \bar{T}_u = \bar{T}_b$, whereas dashed line is for $\bar{T}_l = \bar{T}_b$, $\bar{T}_u = 0$ (or vice versa).

into (2.5), (2.6), the linear term representing vertical advection of the mean temperature field vanishes as $\Delta\bar{T} \to 0$, and the Rayleigh number becomes one (Ra_b) based on $\bar{T}_b$ (to interpret this Rayleigh number physically, we should write it as $(Ra_\delta)/\delta$, where Ra_δ is a Rayleigh number based on the characteristic horizontal temperature variation $\delta\bar{T}_b$ and where it is understood that this ratio remains finite as $\delta \to 0$).

The solution for $\hat{\Theta}$ and $\bar{\Psi}$ can then be obtained by expanding in the manner of (2.9*a*, *b*), after setting $\Delta\bar{T} = 0$. The analysis is then so similar to that given in § 2 that the details are omitted. For case (i), the mean Nusselt number is given in figure 14 as a function of $Ra_b (= Ra_\delta/\delta)$ for various phase angles. The $O(\delta^2)$ mean flow has a profile similar to that given in figure 3. The maximum mean velocity for case (i) is plotted in figure 15 as a function of Ra_b for $\beta = \frac{1}{2}\pi$, which again is the phase angle for the strongest streaming. Other results for the case $\bar{T} = 0$ have been given by Salstein (1974).

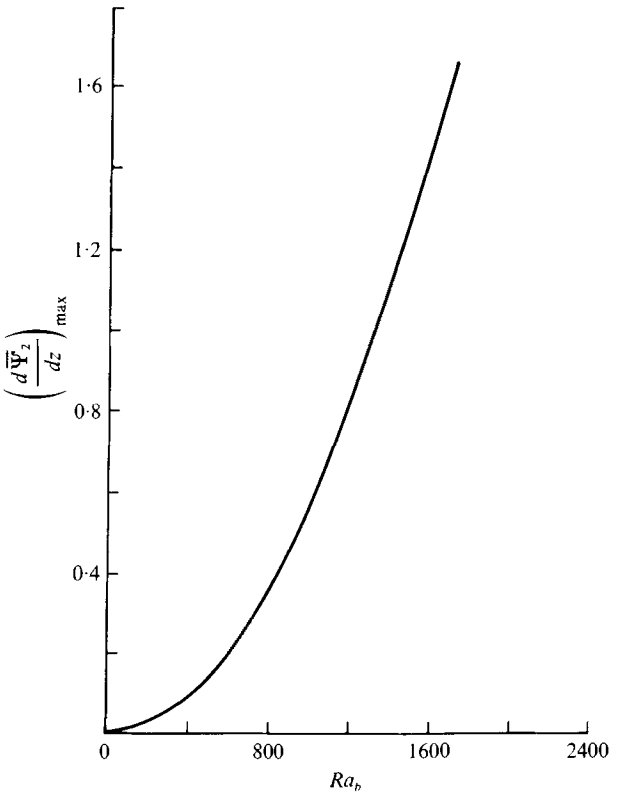

FIGURE 15. Maximum mean velocity at $O(\delta^2)$ for case (i) when $\Delta\overline{T} = 0$, as a function of horizontal Rayleigh number Ra_b and Prandtl number with $\beta = \frac{1}{2}\pi$.

REFERENCES

AHLERS, G. 1975 The Rayleigh–Bénard instability at helium temperatures. *Fluctuations, Instabilities and Phase Transitions* (ed. by T. Riste), pp. 181–193. Plenum.

BUSSE, F. H. 1972 On the mean flow induced by a thermal wave. *J. Atmos. Sci.* **29**, 1423–1429.

CLEVER, R. M. & BUSSE, F. H. 1974 Transition to time-dependent convection. *J. Fluid Mech.* **65**, 625–645.

CHEN, M. N. & WHITEHEAD, J. A. 1968 Evolution of two-dimensional periodic Rayleigh convection cells of arbitrary wave-numbers. *J. Fluid Mech.* **31**, 1–15.

DANIELS, P. G. 1978 The effect of distant sidewalls on the transition to finite amplitude Bénard convection. *Proc. Roy. Soc.* A **358**, 173–197.

DAVIS, S. H. 1976 The stability of time-periodic flows. *Ann. Rev. Fluid Mech.* **8**, 57–74.

FUNG, Y. C. & YIH, C. S. 1968 Peristaltic transport. *J. Appl. Mech., Trans. A.S.M.E.* **35**, 669–675.

HALL, P. & WALTON, I. C. 1978 The smooth transition to a convective regime in a two-dimensional box. *Proc. Roy. Soc.* A **358**, 199–221.

KELLY, R. E. & PAL, D. 1976 Thermal convection induced between non-uniformly heated horizontal surfaces. *Proc.* 1976 *Heat Transfer and Fluid Mech. Inst.*, pp. 1–17. Stanford University Press.

MALKUS, W. V. R. & VERONIS, G. 1958 Finite amplitude cellular convection. *J. Fluid Mech.* **4**, 225–260.

MATKOWSKY, B. J. & REISS, E. L. 1977 Singular perturbations of bifurcations. *SIAM J. Appl. Math.* **33**, 230–255.

PAL, D. & KELLY, R. E. 1978 Thermal convection with spatially periodic nonuniform heating: nonresonant wavelength excitation. *Proc. 6th Int. Heat Transfer Conf. Toronto* (to appear).

SALSTEIN, D. A. 1974 Channel flow driven by a stationary thermal source. *Tellus* **26**, 638–651.

TAVANTZIS, J., REISS, E. L. & MATKOWSKY, B. J. 1978 On the smooth transition to convection. *SIAM J. Appl. Math.* (to appear).

WATSON, A. & POOTS, G. 1971 The effect of sinusoidal protrusions on laminar free convection between vertical walls. *J. Fluid Mech.* **49**, 33–48.

YOUNG, R. E., SCHUBERT, G. & TORRANCE, K. E. 1972 Nonlinear motions induced by moving thermal waves. *J. Fluid Mech.* **54**, 163–187.